AJNR

This information is current as of February 27, 2026.

# Deep medullary veins integrity and relationships with small vessel disease and interstitial diffusivity measures in patients with a recent small subcortical infarct

Carla Brenlla, Caterina Sozzi, Andrés Girona, Emma Muñoz-Moreno, Carlos Laredo, Alejandro Rodríguez-Vázquez, Sergio Amaro, Arturo Renú, Antonio Doncel-Moriano, Laura Llull, Xabier Urra, Salvatore Rudilosso and Ángel Chamorro

*AJNR Am J Neuroradiol* published online 21 November 2024
http://www.ajnr.org/content/early/2024/11/21/ajnr.A8591

This preprint represents the accepted version of the article and also includes the supplemental material; it differs from the printed version of the article.

ORIGINAL RESEARCH

# Deep medullary veins integrity and relationships with small vessel disease and interstitial diffusivity measures in patients with a recent small subcortical infarct

Carla Brenlla[1**], Caterina Sozzi[2**], Andrés Girona[1], Emma Muñoz-Moreno[3], Carlos Laredo[3], Alejandro Rodríguez-Vázquez[4], Sergio Amaro[4], Arturo Renú[4], Antonio Doncel-Moriano[4], Laura Llull[4], Xabier Urra[4], Salvatore Rudilosso[3,4*], Ángel Chamorro [3,4,5].

## ABSTRACT

**BACKGROUND AND PURPOSE:** The role of the venous compartment in cerebral small vessel disease has yet to be fully understood. As such, we evaluated how deep medullary veins integrity relates to MRI-based small vessel disease severity markers and glymphatic function assessed by DTI measures in patients with a recent small subcortical infarct.

**MATERIALS AND METHODS:** We gathered demographic, clinical, and 3 Tesla-MRI imaging data from 50 patients with a recent small subcortical infarct. We evaluate the venular integrity using two visual scales based on their appearance on SWI. We assessed the number of lacunes and microbleeds, white matter hyperintensities volume, perivascular spaces volume in basal ganglia and white matter, summary-small vessel disease score, and brain volume. Diffusivity measures in normal-appearing white matter included free water fraction, mean diffusivity and fractional anisotropy with and without free water correction, and DTI along the perivascular spaces. After categorizing the cohort in quartiles according to both venular scores, we assessed their correlations with small vessel disease markers and diffusivity measures using multivariable ordinal regression analyses adjusting for age, sex, smoking, and summary small vessel disease score.

**RESULTS:** In univariate analysis most of the imaging variables, except for microbleeds, perivascular spaces in white matter and DTI-along the perivascular spaces, were associated with one or both venular scores. In multivariate analysis (OR, 95% CI), free water (1.33, 1.03-1.73), mean diffusivity (4.56, 1.32-15.81), fractional anisotropy (0.77, 0.63-0.93), free water-corrected mean diffusivity and fractional anisotropy (2.39, 1.06-5.39;0.78, 0.65-0.94, respectively), associated with vein appearance, while only brain volume (0.48, 0.25-0.94), fractional anisotropy with and without free water correction (0.82,0.86-0.99; 0.83, 0.7-0.99, respectively) remained significant for vein count.

**CONCLUSIONS:** In patients with a recent small subcortical infarct, disruption of the deep medullary veins, increased extracellular water, and white matter injury appear to be associated.

**ABBREVIATIONS:** SVD=small vessel disease; DMV=deep medullary veins; WMH=white matter hyperintensities; PVS=perivascular spaces; DTI-ALPS=diffusion tensor image analysis along the perivascular spaces; FW=free water; MD=mean diffusivity; FA= fractional anisotropy; BG=basal ganglia.

Received month day, year; accepted after revision month day, year.

[1] Neurology department, Hospital Clínic, Barcelona, Spain.
[2] Neurology department, University of Milano Bicocca, Milano, Italy.
3 August Pi i Sunyer Biomedical Research Institute (IDIBAPS). Barcelona, Spain.
4 Comprehensive Stroke Center, Department of Neuroscience, Hospital Clinic. Barcelona, Spain.
5 University of Barcelona. Faculty of Medicine and Health Sciences. Barcelona, Spain.

**These authors contributed equally.

The authors declare no conflicts of interest related to the content of this article.

**(*)Correspondence:**
Salvatore Rudilosso, Comprehensive Stroke Center, Department of Neuroscience, Hospital Clinic. Barcelona, Spain.
C. de Villarroel, 170, L'Eixample, 08036 Barcelona
+34 627 19 24 11
srudilos@clinic.cat
X: @srudilos82

## SUMMARY SECTION

**PREVIOUS LITERATURE:** Neuropathology studies have revealed the presence of periventricular vein collagenosis in the brains of elderly individuals with white matter disease. Utilizing SWI-MRI sequences, the paramagnetic properties of the venous blood enable vessel visibility in vivo. While visual grading scales based on vein appearance or number have been proposed to evaluate vein integrity, their correlation with other small vessel disease imaging markers remains less defined. Some authors have also suggested a role of venular dysfunction in impeding perivascular flow clearance, leading to stasis of interstitial fluid. However, there is limited evidence of these mechanisms involved in glymphatic function based on DTI measures.

**KEY FINDINGS:** In our cohort, DMV disruption demonstrated a weak association with typical markers of small vessel disease, despite a strong correlation between brain atrophy and reduced vein count. Furthermore, diffusion-based measures indicating microstructural damage and interstitial fluid increase, but not reduced perivenular outflow, exhibited consistently high associations in the multivariable models.



Copyright 2024 by American Society of Neuroradiology.
Copyright 2024 by American Society of Neuroradiology.

**KNOWLEDGE ADVANCEMENT:** We assessed DMV integrity using two methods that correlated well but showed varying associations with other imaging variables. Our findings suggest that DMV integrity may be affected by small vessel disease, influenced by confounding factors. DMV injury is linked to WM integrity and extracellular water content, indicating potential vein dysfunction.

## INTRODUCTION

Cerebral small vessel disease (SVD) primarily affects small penetrating arteries, capillaries, and veins (1). Although most of the research focused on the arterial side pathology, small parenchymal vein collagenosis, characterized by wall sclerosis, leading to venular stenosis and occlusion, may contribute to brain aging and SVD (2,3). Increased vein rigidity and disrupted perivenular fluid flow may lead to interstitial fluid stasis and inefficient metabolism waste clearance (4). However, there is a lack of evidence regarding the clearance of interstitial fluid from the brain deep regions, as it appears to happen predominantly through cortical perivenous spaces (5).

Small parenchymal veins can be evaluated using SWI, a non-invasive MRI technique that exploits the paramagnetic property of deoxyhemoglobin in veins to distinguish them from surrounding brain tissue and arterioles. On SWI axial sections, deep medullary veins (DMV) draining from the periventricular WM (6) are easily visible as thin strips of low signal perpendicular to the lateral ventricle. DMV alterations may be graded using visual scales or quantified by computational segmentation techniques (7). Several studies have attempted to establish a link between the integrity of the DMV on SWI and SVD markers, including WM hyperintensities (WMH), lacunes, microbleeds, perivascular spaces (PVS) (8–15), brain atrophy (9,10), microstructural WM integrity in DTI, extracellular free water (FW) content (16,17), and reduced diffusion along the perivascular spaces (DTI-ALPS index) (13), but the results have been inconsistent. The clinical significance of altered DMV is even weaker, although few studies showed an association with cognitive functions and functional recovery following a stroke (18,19).

We hypothesize that DMV alterations assessed by two visual scales on SWI based on their appearance and count is associated with imaging markers of SVD severity, as well as brain volume, microstructural injury in DTI, and altered brain fluid content and clearance. Therefore, we studied whether two visual DMV scales correlated with SVD severity and diffusivity measures in patients with a recent small subcortical infarct.

## MATERIALS AND METHODS

### *Patients*

The study protocol was approved by the local Ethics Committee (HCB/2023/0748). We followed the STROBE checklist for observational studies (Supplementary material). This is a post-hoc cross-sectional analysis of, a prospective cohort study focused on the relationships between brain diffusivity measures and SVD signatures in patients with lacunar infarct, a common clinical manifestation of SVD. Fifty patients with a recent small subcortical infarct were admitted between June 2022 and March 2023 and underwent appropriate diagnostic workup. No patients had a known demyelinating disease. The presence of a recent small subcortical infarct confirmed on DWI sequences according to the STandards for ReportIng Vascular changes on nEuroimaging (STRIVE) criteria (20) was mandatory for the enrolment. The exclusion criteria were contraindications for MRI, severe dependency, and presence of brain lesions other than those related to SVD that could interfere with the imaging analysis, such as large infarcts or space-occupying lesions. Investigational 3-Tesla MRI was acquired at least 4 weeks after the infarct identified at enrolment. A neurologist (SR) reviewed the quality of SWI sequences, which were all suitable for the analyses. The collected variables included age, sex, number of cigarettes per day, history of hypertension, diabetes and hyperlipidemia.

### *Investigational MRI acquisition*

All MRI studies were acquired at the IDIBAPS MRI Core Facility with a 3T-MRI scanner (MAGNETOM Prisma, Siemens Healthineers, Erlangen, Germany) with a 32-channel phased-array coil. During scanning, a technician evaluated the image quality and repeated the sequence acquisition if necessary. The image acquisition protocol, according to HARmoNizing Brain Imaging MEthodS for VaScular Contributions to Neurodegeneration (HARNESS) (21), included the following sequences: 3D T1 (1.0x1.0x1.0 mm3, matrix 256x256, FOV 256x256 mm², 192 slices, TR/TE/TI 2500/4.37/1100 ms); 3D T2 (0.9x0.9x0.9 mm3, matrix 256x256, FOV 240x240 mm², 176 slices, TR/TE 3200/406 ms); 3D FLAIR (0.5x0.5x1.0 mm3, matrix 512x512, FOV 256x256 mm², 192 slices, TR/TE/TI 5000/388/1800 ms); SWI (0.6x0.6x3 mm3, matrix 312x384, FOV 195x240, 52 slices, TR/TE 28/20 ms); DWI, 2.0x2.0x2.0 mm3, matrix 112x112, FOV 224x224 mm², 76 slices, TR/TE 3000/113 ms, 14 baseline images acquired (b-value=0) and three shells with b-values 500 s/mm², 1000 s/mm², 2000 s/mm² and 6, 64 and 64 gradient directions respectively).

### *Visual assessment of DMV on MRI*

We used two visual scales to assess the DMV on SWI (Figure 1). The first scale by Zhang et al.(8), which we will refer to as appearance-DMV, is based on DMV aspect (Figure 2). The protocol was adjusted from the original version to accommodate the differing slice thickness and voxel sizes (3mm instead of 2mm of the original protocol). We identified 3 contiguous periventricular slices (each 3 mm thick) from the level immediately superior to the basal ganglia (BG) to the level where the ventricles disappear in each patient. Furthermore, each slice is subdivided into six regions, encompassing the frontal, parietal, and occipital areas on both sides, where DMV appearance was graded as follows: Grade 0: all veins are continuous with homogeneous signal. Grade 1: each vein is continuous, but one vein or more has an

inhomogeneous signal. Grade 2: one vein or more is not continuous with spot-like hypointensity. Grade 3: none of the veins are continuous. Finally, the 6 scores are summed into an overall score that ranges from 0 (completely normal) to18 (hardly visible unstructured veins).

The second scale by Ao et al. (9) (Figure 1), which we will refer to as count-DMV, is based on the count of visible DMV on MIP-SWI sequences setting a ROI in each cerebral hemisphere in the periventricular WM between the frontal and the occipital horn, and from the ventricle floor to the superior roof of the corpus callosum. The count-DMV score is the average count of both hemispheres. After training on 20 patients from clinical practice scans, two raters, a vascular neurologist with a 10-year experience (SR), and a Neurology trainee (CB), independently evaluated both scores for the study cohort. Discordances in DMV-appearance scores were discussed to assign the final score, while count-DMV scores were averaged.

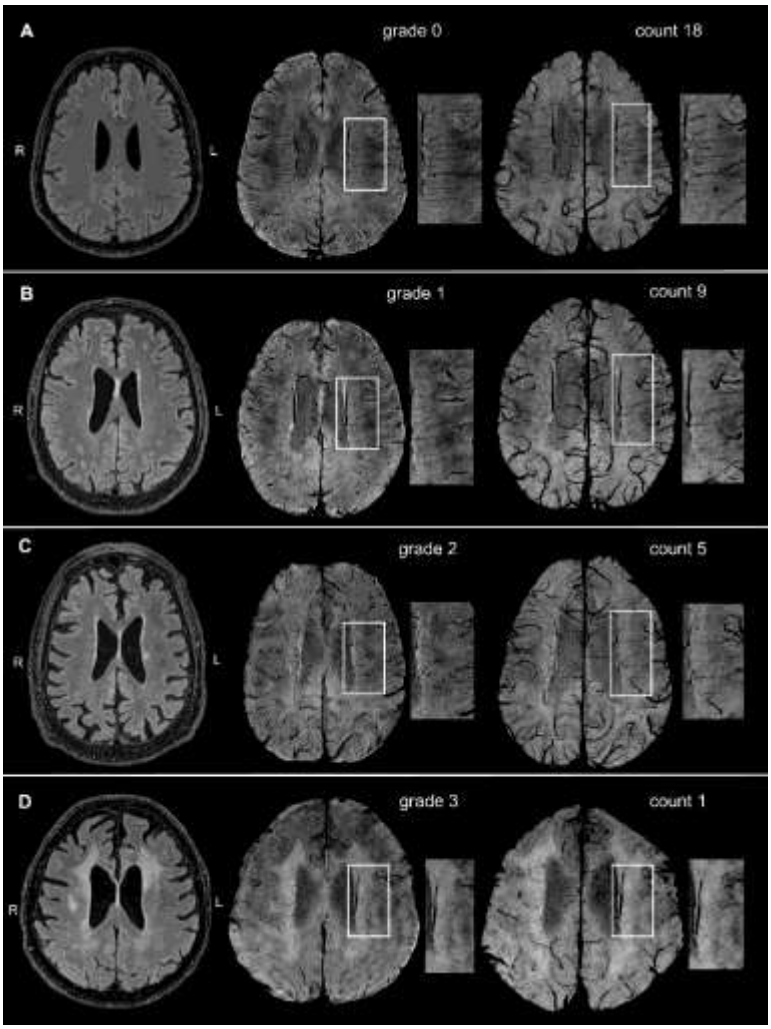


**FIG 1.** Examples of DMV assessment methods. The left column shows the different degrees of SVD on FLAIR sequences; the middle column represents the appearance-DMV score on SWI sequences, the right column represents the corresponding count in the left hemisphere on MIP sequences. (A) Male, 64 years. There are no visible signs of WMH on FLAIR, on SWI each vein is continuous and has quite a homogeneous signal (grade 0) and on MIP a total of 18 veins can be counted. (B) Male, 74 years. No visible signs of SVD on FLAIR sequence, each vein is continuous but at least there is one with inhomogeneous signal (grade 1) and we count 9 veins in the left hemisphere. (C) Male, 84 years. There are some non-confluent WMH on FLAIR (Fazekas grade 1), at least one vein is not continuous with a spot-like hypointensity (grade 2), while the total number of veins is 5. (D) Male, 70 years. There are large confluent WMH, none of the veins are continuous (grade 3) on SWI and only one vein can be counted on MIP.

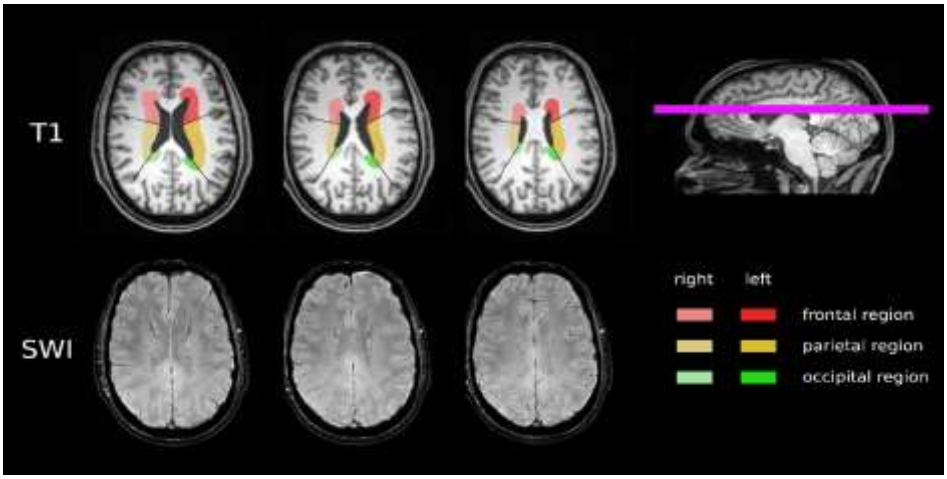


**FIG 2.** Visual assessment for DMV appearance on SWI, based on Zhang et al. The protocol was tailored for SWI sequences with a 3 mm thickness. Three continuous periventricular sections were chosen, as indicated by the pink bar on the sagittal section on the right side of the panel. Each section was subdivided into six regions (depicted in different colours), encompassing frontal, parietal, and occipital areas on both sides. A score ranging from 0 (indicating a completely normal and homogenous appearance of DMV) to 3 (indicating highly disorganized and nearly invisible DMV) is assigned to each region. The sum of the scores from all regions yields the final score (ranging from 0 to 18). The upper row of T1-weighted images shows the anatomical details of the selected regions, while the lower row of SWI sections demonstrates the appearance of the DMV for visual evaluation.

### *SVD assessment on MRI*

The typical SVD markers were defined according to STRIVE criteria(20). The summary SVD score (range 0-4), accounts for the presence of ≥1 lacunes, ≥1 cerebral microbleeds, PVS grade in BG ≥2 and WMH with Fazekas score ≥2 in deep WM or periventricular Fazekas score =3 (22).

For the PVS segmentation we used a semiautomated method applying the Frangi filter to T2-weighted image (Figure 3) (23). We applied a filter removing small clusters of 5 or fewer voxels (3.65 $mm^3$), mostly due to background noise, and removed regions corresponding to lacunes and infarcts. Since PVS have distinct anatomical and functional features depending on their location (20), we selected two main regions for PVS quantification, defined as WM (frontal, parietal, temporal and occipital lobes, excluding fiber tracts between BG) and BG (lenticular nucleus, caudate, thalamus, internal and external capsule). We obtained the fractional PVS volume for each of the two subtypes, by normalizing the BG PVS to the total BG volume, and the WM PVS to the WM volume (24,25). We segmented the WMH using a method based on Valdés-Hernández et al. (25) on the 3D FLAIR sequence. A prior lesion space is registered to the subject FLAIR sequence, and specific thresholds are applied to identify the hyperintensities. Areas identified as lacunes or strokes were removed. All segmentations were checked and edited if required (SR). For all analyses, we used the WMH ratio defined as WMH volume/intracranial volume. Total brain volume was obtained by FreeSurfer quantification.

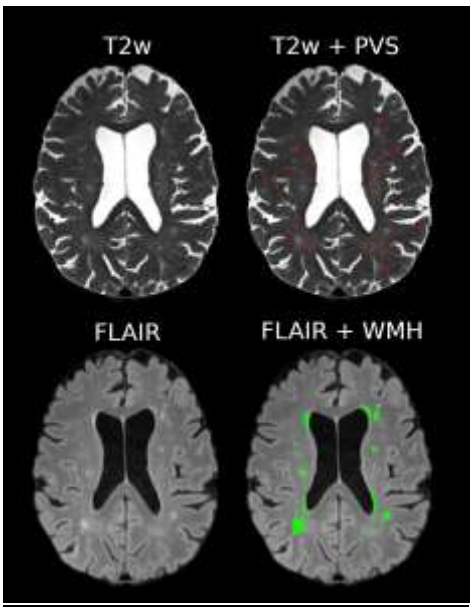


**FIG 3.** PVS and WMH segmentation methods. The figure displays an axial section at the level of the centrum semiovale from a 76-year-old male patient. PVS and WMH are depicted on T2-weighted and FLAIR sequences, respectively.

### *Brain diffusivity analysis*

DTI measures were obtained from normal-appearing WM to avoid skewed values due to macrostructural damage in WMH or infarcts. The DTI-ALPS index (ratio of diffusivity in the direction of the PVS to the diffusivity perpendicular to the major fiber tracts) estimates interstitial fluid dynamics along PVS that align with medullary veins (26). For the analysis, we used the DTI-ALPS index from the non-infarct side. Multi-shell DWI was processed using dipy (27). Preprocessing includes correction of eddy currents and distortion using topup, denosining and skull stripping. For DTI-ALPS estimation a diffusion tensor model was fitted to the preprocessed image. FA and MD were obtained from the DTI. Color-FA map was obtained and used to manually identify the regions of interest for DTI-ALPS index computation. Besides, a free water elimination model was also fitted to the pre-processed diffusion images to obtain the FW-corrected MD and FW-corrected FA, as well as the estimated FW fraction. All these parameters (FA, FW, FW-corrected MD, and FW-corrected FA) were averaged in the subcortical normal appearing-WM after excluding SVD lesions. To assess the consistency of diffusion measures, we analyzed their distribution using density plots, revealing consistent patterns across the cohort (Supplementary figure 1).

### *Statistical analysis*

To assess inter-rater reliability for DMV scores, we used the intraclass correlation coefficient and Bland-Altman's plots. After assigning the final scores, we analyzed the correlations using Spearman's coefficient between appearance-DMV scores from distinct brain regions. We assessed the correlations of DMV counts in relation to laterality (left/right) and to the infarct side. The presence of a linear association between the two DMV scores was analyzed by a scatter plot.

For the cohort description, we utilized absolute frequency and proportion for categorical data, means and standard deviation (SD) for normally distributed continuous variables, and median and interquartile ranges (IQRs) for non-parametric variables. Given the skewed distribution of DMV scores, we stratified the cohort into DMV scores quartiles. Then, we analyzed the distribution of the variables amongst DMV scores quartiles, identifying differences using ANOVA or Kruskall-Wallis test, as appropriate.Variables showing significant differences among quartiles were further examined using multivariable ordinal regression, using the least pathological quartile in DMV scores as the reference standard. Therefore, since the two scales had an inverse trend according to DMV disruption, we used inverse count-DMV quartiles (1$^{st}$ quartile had the highest DMV count). The regression models were adjusted for pre-established relevant confounders and those with P < .1 in the univariate analyses. Model 1 included age, sex, and cigarette number; Model 2 added summary-SVD score to Model 1.

We considered statistically significant values of P<.05, and all hypotheses were 2-sided. Analyses were calculated in Stata v15 for MacOS and v18.0 for Windows 11 (College Station, TX: StataCorp LLC). The STATA syntaxis is available in: https://github.com/carlabrenlla/DMV-study.git. We considered that this exploratory analysis, conducted in a limited sample, could reveal relevant associations based on prior observations in the same cohort between FW and SVD markers (unpublished).

## RESULTS

### *General features of the study cohort*

All fifty patients had complete data, including suitable SWI sequences. Eighteen participants (36%) were females, the median age was 71.4 (IQR 64.7-77.6) years. Most of the participants had history of hypertension (62%) and hyperlipidemia (58%), and seventeen (34%) had diabetes mellitus. Eighteen subjects (36%) were current smokers. The median summary SVD score of 2 (IQR 1-3) reflects that SVD signatures were highly represented in this cohort.

### *DMV reliability assessment and description*

The intraclass correlation coefficient for the appearance-DMV score (95% CI) was 0.79 (0.73-0.85) without any systematic bias in Bland-Altman's plot (Figure 4.A). The Spearman coefficients between scores from different regions and sides ranged between 0.66 and 0.71 (P<.001) (Table 1), and was 0.868 (p<0.001) comparing the infarct vs. contralateral side. After solving discordances, the median appearance-DMV score was 11 (IQR 9-14).

As for the count-DMV scale, the intraclass correlation coefficient (95% CI) for left and right side was 0.83 (0.69-0.90) and 0.81 (0.67-0.90), respectively, without any systematic bias in Bland-Altman's plot (Figure 4.B).

After averaging raters' scores, the median count-DMV for each side was 6 (IQR 3-8.5), without asymmetry (mean difference, SD, P) according to infarct laterality (0.22, 2.2, P=.48) and left/right side (0.38, 2.2, .22). The appearance-DMV score accounted for 56% of the variation in count-DMV score (F (1, 48) =61.94; b=-0.65; P<.001) (Figure 5), and the Spearman's correlation between the two scales was rho= -0.6875, p<0.001.

We did not observe any significant difference in clinical variables among quartiles of the 2 DMV scales (Online Supplemental Data). Among radiological variables, there were differences in WMH volume (p=0.002) and brain volumes (p<0.02) using both DMV scales, in PVS in BG (p=0.015) and summary-SVD score (p=0.036) using appearance-DMV scores. All DTI measures except for DTI-ALPS index had differences in quartiles distribution using appearance-DMV (p<0.018), while only MD, and FA, and FW-adjusted FA showed significant differences between count-DMV quartiles. These most relevant distributions are represented in Supplementary figure 2.

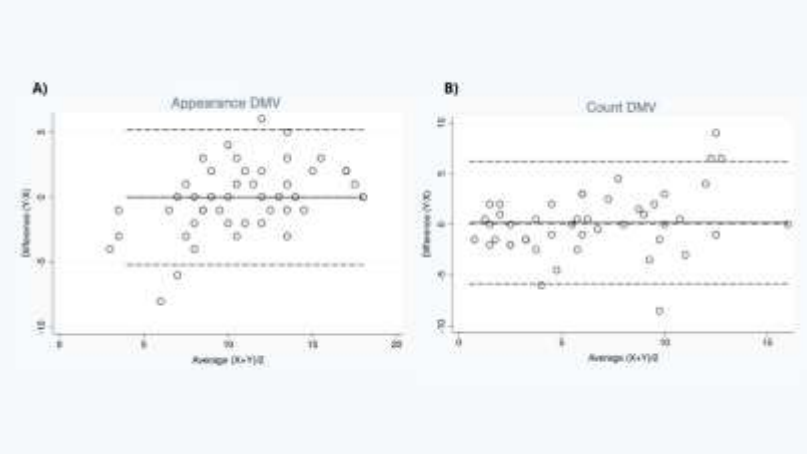


**FIG 4.** Bland-Altman's plots. Interrater agreement between the original scores from 2 observers, according to appearance-DMV (A) and count-DMV scales (B), respectively.

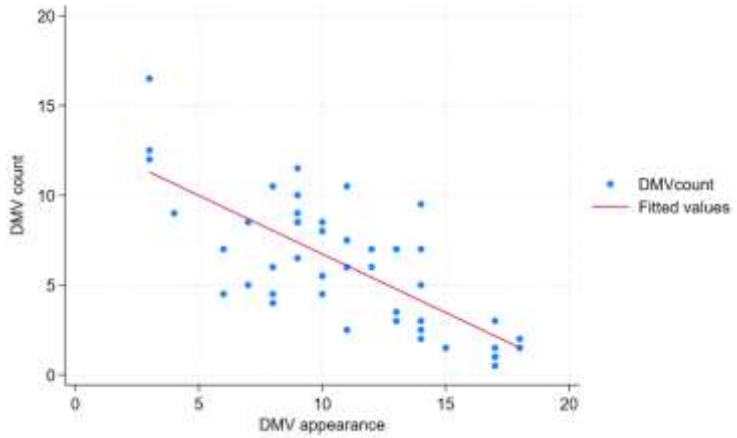


**FIG 5.** Association between the appearance-DMV and count-DMV scales. Linear regression analysis where the appearance-DMV score accounted for 56% of the variation of count-DMV score (F (1, 48) = 61.94; b=-0.65; 95% CI: -0.82 to -0.49; P<.001).

**Table 1**: Correlation between appearance-DMV score in different brain regions.

| **Spearman's correlation coefficients between left DMV regions** | | |
|---|---|---|
| | Left parietal | Left occipital |
| Left frontal | r = 0.70 | r = 0.67 |
| Left parietal | r = 1 | r = 0.66 |
| **Spearman's correlations coefficients between right DMV regions** | | |
| | Right parietal | Right occipital |
| Right frontal | r = 0.71 | r = 0.71 |
| Right parietal | r = 1 | r = 0.69 |

### *Ordinal univariate and multivariate regression analyses*

In the ordinal regression analyses (OR, 95% CI) using appearance-DMV as the dependent variable, reduced brain volume (0.5, 0.31–0.8), WMH ratio (1.73, 1.11-2.71), PVS in BG (1.43, 1.01-1.94) and summary SVD score (1.64, 1.06-2.54), were associated with a higher score only in the unadjusted model; FW-corrected MD only in model 2 (2.39, 1.06-5.39); FW, MD, FA, and FW-corrected FA in all models (model 2: 1.33, 1.03-1.73; 4.56, 1.32-15.81; 0.77, 0.63-0.93; 0.78, 0.65-0.94; respectively) (Figure 6, Supplementary table 2).

In the ordinal regression analyses (OR, 95% CI) using count-DMV as the dependent variable, WMH ratio (1.99, 1.21-3.26), number of lacunes (1.26, 1.01-1.58), summary SVD score (1.65, 1.09-2.48) and FW in normal appearing-WM (1.34, 1.07-1.68) were associated with a higher score only in the unadjusted model; reduced brain volume, FA and FW-corrected FA in all models (model 2: 0.48, 0.25-0.94; 0.82, 0.68-0.99; 0.83, 0.7-0.99; respectively) (Figure 6, Supplementary table 2).

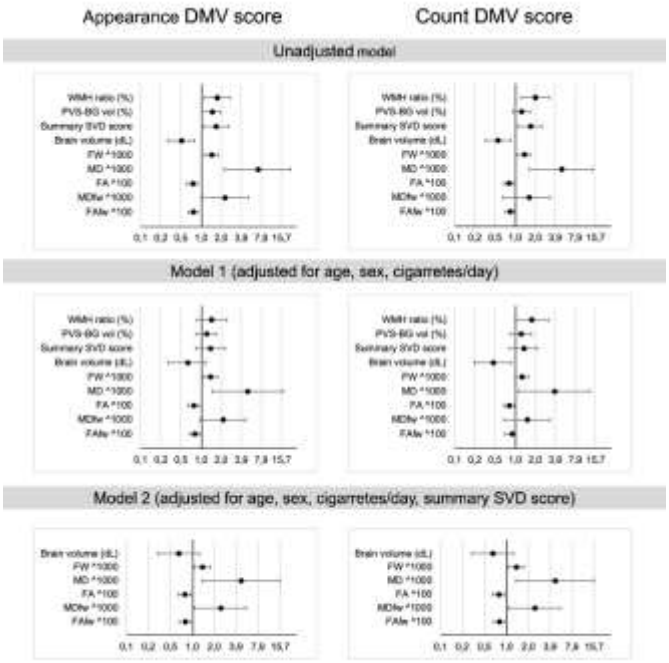


**FIG 6.** Forest plots of the variable with a significant association in the ordinal regression analyses, using either appearance-DMV score or count DMV score as the dependent variable.

## DISCUSSION

The results of our study align with previous evidence that DMV integrity may be linked to other SVD features (8–15). However, these relationships are complex and contingent upon varying methods used to assess DMV. Scores indicating DMV disruption showed a strong relationship with microstructural WM integrity and FW content, suggesting the potential involvement of extracellular fluid in mechanisms leading to vein disruption.

The two visual scores showed consistent agreement between observers, which could be partially due to prior training. Despite a linear correlation, one scale explained only 56% of the variation in the other, indicating that they are not interchangeable. The appearance-DMV scale showed strong correlations across brain regions and sides, suggesting that the 6-region scoring system could be simplified to a single qualitative score. The count-DMV score is less challenging, but overlooks loss of signal homogeneity, which could reflect early structural or functional changes. Therefore, the appearance DMV could better capture signal alteration due to venular collagenosis-related stenosis, without affecting the vein count, while count-DMV score could not be a sensitive marker of DMV integrity.

Overall, the correlations between DMV disruption and SVD markers point towards loss of venous integrity despite not reaching statistical significance in adjusted models, due to the limited sample size. As regards WMH volume, it was associated with higher DMV scores in unadjusted analysis, but not after adjusting for covariates, despite maintaining a similar trend. Age and vascular risk factors may attenuate the association between DMV and WMH volume, as suggested by inconsistent evidence from larger cohorts (9,13), possibly due to high heterogeneity in study populations, WMH volume assessment, and multivariable models. PVS volume in BG, and lacunes, showed a weak association with appearance DMV scores that was no longer significant in adjusted models. Notably, DMV scores showed no trends with PVS volume in WM. Other works showed relationships between PVS in BG (12,15) but none found a relationship between DMV and PVS in WM. These results support the hypothesis that PVS are mainly periarterial (24) and that their enlargement in BG may be due mainly to hypertensive injury, while in lobar WM, amyloid deposition and impaired glymphatic clearance may play a significant role (1). Similarly, the summary SVD score, as a global measure of small vessel damage, was associated with both DMV scores only in unadjusted models. However, more consistent associations have been demonstrated in larger cohorts (11,14).

Brain atrophy is a common SVD feature (20) and was associated with fewer DMVs in all models, while not reflecting worse DMV appearance. These findings may be attributed to decreased metabolism and perfusion associated with neuronal loss and demyelination, which are characteristic of the aging and neurodegenerative-related processes (28). These findings confirm previous evidence of reduced brain volume in subjects with low DMV number or density (9,29–31), while the association with altered vein morphology remains

controversial (10).

We observed strong associations between diffusion metrics and DMV scores, suggesting that early injury in the normal appearing-WM might be present when DMV are affected in SVD, as previously described (16,17). Patients with higher DMV scores exhibited increased MD and decreased FA. Moreover, we noted increased FW among patients with diminished DMV integrity. Notably, while FW-corrected FA showed a significant association with higher DMV scores, FW-corrected MD did not. These changes indicate fiber demyelination (resulting in decreased FA and FW-corrected FA) and increased edema, or insufficient extracellular water clearance (increased FW)(32). Finally, DTI-ALPS index showed no relationships with DMV scores, suggesting that the diffusivity along the venular PVS is not compromised. However, the results from a community population study showed an inverse association between DTI-ALPS index and DMV disruption(13). These diverging findings warrant further investigation since the DTI-ALPS methodology might not capture water clearance entirely (33).

Significant correlations between DMV scores and clinical variables were not found, except for an almost significant association with age which might be clinically relevant considering the limited age range and high prevalence of risk factors in our sample. Noteworthy, the inclusion of age in multivariable models attenuated the association between DMV and other SVD markers. Larger studies have established DMV integrity associations with age (9), hypertension(10) and cognitive tests (18). The possible link between the DMV number and smoking is underexplored and warrants further confirmation.

This study has some relevant strengths. Differing from prior studies, we conducted a thorough analysis of DMV integrity using two different DMV evaluation methods and a complete assessment of SVD markers, including brain volume an DTI-based measures. MRI acquisition protocols were set up according to HARNESS recommendations for investigation in SVD (21). The WMH and PVS quantification was conducted using validated algorithms and revised manually. The scores for DMV underwent independent evaluation before their utilization in the primary analyses.

There are also some important limitations. Firstly, the small sample size might not have been sufficient to depict significant associations in multivariable models, when considering the cumulative impact of risk factors commonly coexisting in SVD. Secondly, the absence of quantitative DMV assessment via segmentation methods, which are challenging to apply to our SWI prtocol (7), limits our analysis of vessel length and tortuosity. Thirdly, differences in vessel visibility on SWI may be due to factors other than venular collagenosis-related changes, such as the presence of other paramagnetic substances, temperature, pH, blood flow, and vessel orientation, tortuosity and anatomical variability, which can confound the assessment of DMV appearance (34). Although we controlled for potential factors related to MRI acquisition, by using the same protocol and scanner for all subjects, the SWI slice thickness of 3mm may have reduced the accuracy due to partial volume effects that could lead to false positives for vessel discontinuity. Moreover, the accuracy of DTI metrics could have been affected by the voxel size in multi-shell DWI, which may lead to partial volume effects. Finally, while our results suggest that DMV integrity is a potential marker of SVD, whether it plays an etiological role in the development of its pathogenic role in SVD and its clinical and radiological progression, needs assessment through larger longitudinal studies, including longitudinal and neuropathological studies.

Further research is needed to validate the DMV assessment on SWI, which should include post-mortem brain examination, high-resolution SWI to improve the accuracy of subjective DMV assessment and allow automated segmentation. Studies at 7T would allow better visualization of medullary veins on SWI, due to the higher resolution that can be achieved and greater susceptibility effects at ultra-high field strength, and also allow more accurate automated segmentation of DMV (35). Additionally, the analysis of vascular brain functions might provide useful data on,–perfusion, pulsatility, cerebrovascular reactivity, and oxygen extraction, according to DMV integrity (20). Due to the limited availability of vein segmentation methods for 1.5 or 3T MRI, there is a need for a simpler visual assessment method to evaluate DMV appearance, which could be based on a global qualitive scale for the periventricular WM. Future studies should evaluate the reliability and precision of such practical approach that could find easier application in clinical settings or in sizable research studies.

## CONCLUSIONS

In patients with a recent small subcortical infarct, DMV may be affected in number or morphology. Despite the weak associations with typical SVD features, DMV alterations are associated with microstructural damage and increased extracellular water (FW), but not impaired fluid clearance measures (DTI-ALPS index). This suggests an imbalance in interstitial fluid regulation without a noticeable reduction in perivenular water molecule diffusivity. The assessment of the venous compartment has the potential to advance the comprehension of the pathophysiological mechanisms underpinning SVD. However, more research is needed to establish reliable methods for assessing DMV pathology and its clinical significance before considering DMV alterations on MRI as a reliable marker of SVD.

## ACKNOWLEDGMENTS

Project funded by the Catalan Society of Neurology (2001, https://www.scneurologia.cat/beca-fundacio-societat-catalana-de-neurologia/) and by a grant from the Carlos III Health Institute (ISCIII) co-funded by the European Union (PI22/00771). SR receives funding from ISCIII (JR21/00011); AR from ISCIII (PI20/00901); XU from ISCIII (INT22/00043), and by the European Social Fund «The ESF–Investing in your future». This work was partially developed at the building Centro Esther Koplowitz, Barcelona, CERCA Programme/Generalitat de Catalunya. This work was performed thanks to the 3T MRI equipment at IDIBAPS (grant IBPS15-EE-3688 confunded by MINECO and ERDF).

REFERENCES


1. Wardlaw JM, Smith C, Dichgans M. Small vessel disease: mechanisms and clinical implications. Lancet Neurol. 2019 Jul 1;18(7):684–96
2. Moody DM, Brown WR, Challa VR. Periventricular venous collagenosis: association with leukoaraiosis. Radiology. 1995;194(2):469–76.
3. Nan D, Cheng Y, Feng L. Potential Mechanism of Venous System for Leukoaraiosis: From post-mortem to in vivo Research. Neurodegener Dis. 2019;19(3–4):101–8.
4. Bohr T, Hjorth PG, Holst SC. The glymphatic system: Current understanding and modeling. iScience. 2022;25(9).
5. Sennfält S, Thrippleton MJ, Stringer M. Visualising and semi-quantitatively measuring brain fluid pathways, including meningeal lymphatics, in humans using widely available MRI techniques. Journal of Cerebral Blood Flow and Metabolism. 2023;43(10):1779–95.
6. Taoka T, Fukusumi A, Miyasaka T. Structure of the Medullary Veins of the Cerebral Hemisphere and Related Disorders. Radiographics. 2017;37(1):281–97.
7. Bouvy WH, Biessels GJ, Kuijf HJ. Visualization of perivascular spaces and perforating arteries with 7 T magnetic resonance imaging. Invest Radiol. 2014;49(5):307–13.
8. Zhang R, Zhou Y, Yan S. A Brain Region-Based Deep Medullary Veins Visual Score on Susceptibility Weighted Imaging. Front Aging Neurosci. 2017;9(AUG)
9. Ao DH, Zhang DD, Zhai FF. Brain deep medullary veins on 3-T MRI in a population-based cohort. J Cereb Blood Flow Metab. 2021;41(3):561–8.
10. Chen X, Wei L, Wang J. Decreased visible deep medullary veins is a novel imaging marker for cerebral small vessel disease. Neurol Sci. 2020;41(6):1497–506.
11. Yin X, Han Y, Cao X. Association of deep medullary veins with the neuroimaging burden of cerebral small vessel disease. Quant Imaging Med Surg. 2023;13(1):27–36.
12. Wang X, Lyu J, Duan Q. Deep medullary vein damage correlates with small vessel disease in small vessel occlusion acute ischemic stroke. Eur Radiol. 2024.
13. Cai J, Sun J, Chen H. Different mechanisms in periventricular and deep white matter hyperintensities in old subjects. Front Aging Neurosci. 2022.
14. Xu Z, Li F, Wang B. New Insights in Addressing Cerebral Small Vessel Disease: Association With the Deep Medullary Veins. Front Aging Neurosci. 2020.
15. Zhang K, Zhou Y, Zhang W. MRI-visible perivascular spaces in basal ganglia but not centrum semiovale or hippocampus were related to deep medullary veins changes. J Cereb Blood Flow Metab. 2022.
16. Zhang R, Huang P, Jiaerken Y. Venous disruption affects white matter integrity through increased interstitial fluid in cerebral small vessel disease. J Cereb Blood Flow Metab. 2021.
17. Wang H, Lei X, Lan H. Impact of Decreased Visibility of Deep Medullary Veins on White Matter Integrity in Patients with Cerebral Small Vessel Disease. J Integr Neurosci. 2023.
18. Liao M, Wang M, Li H. Discontinuity of deep medullary veins in SWI is associated with deep white matter hyperintensity volume and cognitive impairment in cerebral small vessel disease. J Affect Disord. 2024.
19. Chen X, Luo Y, Zhang S. Deep medullary veins: a promising neuroimaging marker for mild cognitive impairment in outpatients. BMC Neurol. 2023.
20. Duering M, Biessels GJ, Brodtmann A. Neuroimaging standards for research into small vessel disease-advances since 2013. Lancet Neurol. 2023.
21. Smith EE, Biessels GJ, De Guio F. Harmonizing brain magnetic resonance imaging methods for vascular contributions to neurodegeneration. Alzheimers Dement (Amst). 2019.
22. Staals J, Makin SDJ, Doubal FN. Stroke subtype, vascular risk factors, and total MRI brain small-vessel disease burden. Neurology. 2014.
23. Duarte Coello R, Valdés Hernández M del C, Zwanenburg JJM. Detectability and accuracy of computational measurements of in-silico and physical representations of enlarged perivascular spaces from magnetic resonance images. J Neurosci Methods. 2024.
24. Valdés Hernández MDC, Ballerini L, Glatz A. Step-by-step pipeline for segmenting enlarged perivascular spaces from 3D T2-weighted MRI, 2018-2023. University of Edinburgh; 2023
25. Valdés Hernández MDC, Ferguson KJ, Chappell FM. New multispectral MRI data fusion technique for white matter lesion segmentation: method and comparison with thresholding in FLAIR images. Eur Radiol. 2010 Jul;20(7):1684–91.
26. Taoka T, Masutani Y, Kawai H. Evaluation of glymphatic system activity with the diffusion MR technique: diffusion tensor image analysis along the perivascular space (DTI-ALPS) in Alzheimer's disease cases. Jpn J Radiol. 2017 Apr;35(4):172–8.
27. Garyfallidis E, Brett M, Amirbekian B, et al. Dipy, a library for the analysis of diffusion MRI data. Front Neuroinform. 2014 Feb 21;8(FEB)
28. Huang CW, Hsu SW, Chang YT. Cerebral Perfusion Insufficiency and Relationships with Cognitive Deficits in Alzheimer's Disease: A Multiparametric Neuroimaging Study. Sci Rep. 2018 Dec 1;8(1).

29. Liu ZY, Wang P, Zhai FF. Dynamic Mechanism of Cerebral Venous Disruption: Longitudinal Evidence From a Community-Based Cohort. J Am Heart Assoc. 2024;13(10)

30. Liu ZY, Zhai FF, Ao DH. Deep medullary veins are associated with widespread brain structural abnormalities. J Cereb Blood Flow Metab. 2022;42(6):997–1006.

31. Li C, Rusinek H, Chen J. Reduced white matter venous density on MRI is associated with neurodegeneration and cognitive impairment in the elderly. Front Aging Neurosci. 2022;14

32. Duering M, Finsterwalder S, Baykara E. Free water determines diffusion alterations and clinical status in cerebral small vessel disease. Alzheimers Dement. 2018;14(6):764–74.

33. Ringstad G. Glymphatic imaging: a critical look at the DTI-ALPS index. Neuroradiology. 2024;66(2):157–60.

34. Hermier M, Nighoghossian N. Contribution of susceptibility-weighted imaging to acute stroke assessment. Stroke. 2004;35(8):1989–94.

35. Kuijf HJ, Bouvy WH, Zwanenburg JJM, et al. Quantification of deep medullary veins at 7 T brain MRI. Eur Radiol. 2016 Oct 1; 26(10):3412–8

## SUPPLEMENTAL FILES

**Online Supplemental Data**: Descriptive analysis according to the appearance-DMV score quartiles and count-DMV, respectively.

| | **Appearance-DMV score** | | | | | **Count-DMV score** | | | | |
|---|---|---|---|---|---|---|---|---|---|---|
| | **Q1** | **Q2** | **Q3** | **Q4** | **P** | **Q1** | **Q2** | **Q3** | **Q4** | **P** |
| **Clinical and demographic variables** | | | | | | | | | | |
| Age, years, median (IQR) | 65.1 (57.6-75) | 73.8 (61.3-79.9) | 78.7 (67.7-83.2) | 67.6 (66.2-71.9) | .06 | 69.7 (59.4-77.6) | 72.9 (63.0-77.7) | 74.9 (57.6-79.9) | 67.6 (66.0-71.9) | .92 |
| Females, *n* (%) | 4 (22.2%) | 6 (54.6%) | 5 (41.7%) | 3 (33.3%) | .35 | 1 (10%) | 4 (33.3%) | 7 (50%) | 6 (42.9%) | .22 |
| Cigarettes per day, median (IQR) | 0 (0-10) | 0 (0-8) | 0 (0-2) | 0 (0-5) | .87 | 0 (0-0) | 0 (0-0) | 0 (0-20) | 4.5 (0-10) | .06 |
| Hypertension, *n* (%) | 8 (44.4%) | 9 (81.8%) | 9 (75%) | 5 (55.6%) | .16 | 5 (50%) | 7 (58.3%) | 11 (78.6%) | 8 (57.1%) | .48 |
| Mellitus Diabetes, *n* (%) | 3 (16.7%) | 4 (36.4%) | 5 (41.7%) | 5 (55.6%) | .20 | 4 (40%) | 3 (25%) | 4 (28.6%) | 6 (42.9%) | .74 |
| Hyperlipidemia, *n* (%) | 11 (61.1%) | 7 (63.6%) | 5 (41.7%) | 6 (88.7%) | .61 | 5 (50%) | 7 (58.3%) | 8 (57.1%) | 9 (64.3%) | .92 |
| **Radiological variables** | | | | | | | | | | |
| Number of lacunes, median (IQR) | 0.5 (0-1) | 3 (1-6) | 1 (0-2.5) | 2 (0-4) | .11 | 1 (0.5-1) | 1 (0.5-1) | 2 (0-6) | 2.5 (1-4) | .23 |
| Number of microbleeds, median (IQR) | 0 (0-0) | 0 (0-1) | 0 (0-0) | 0 (0-2) | .10 | 0 (0-0) | 0 (0-0) | 0 (0-1) | 0 (0-1) | .47 |

| | | | | | | | | | | |
|---|---|---|---|---|---|---|---|---|---|---|
| WMH ratio, median (IQR) | 0.3 (0.2-0.6) | 1.1 (0.4-2.2) | 0.9 (0.6-3.2) | 1.4 (0.5-1.8) | .002* | 0.3 (0.2-0.6) | 0.4 (0.3-0.8) | 1.3 (0.7-2.3) | 1.2 (0.5-2.4) | .002* |
| PVS-BG, median (IQR) | 2.8 (1.6-3.9) | 4.5 (3.3-6.1) | 4.4 (3.1-4.9) | 3.5 (3.0-5.7) | .015* | 3.2 (1.6-4.5) | 3.5 (3-4.3) | 4.0 (2.6-6.1) | 3.4 (2.9-5.7) | .67 |
| PVS-WM, median (IQR) | 0.5 (0.3-0.7) | 1.0 (0.4-1.9) | 0.7 (0.3-1.2) | 0.7 (0.5-1.1) | .24 | 0.4 (0.3-1.4) | 0.6 (0.4-1) | 0.6 (0.2-1.8) | 0.7 (0.4-1.1) | .90 |
| Summary SVD score, median (IQR) | 1.5 (0-2) | 3 (2-4) | 2.5 (1.5-3) | 3 (1-3) | .036* | 1.5 (0-3) | 2 (0.5-2.5) | 3 (1-3) | 3 (2-3) | .09 |
| Brain volume (mL), median (IQR) | 1068.8 (964-1210.5) | 988.7 (922-1011.4) | 941.2 (880.5-704.4) | 986.4 (897.4-993.7) | .02* | 1138.5 (1008-1210.5) | 1013.7 (960.6-1049.6) | 940.9 (885.2-988.7) | 988 (897-1011.4) | .01* |
| ALPS index, mean (SD) | 1.4 (0.2) | 1.4 (0.2) | 1.4 (0.2) | 1.4 (0.3) | .98 | 1.4 (0.2) | 1.5 (0.2) | 1.3 (0.2) | 1.4 (0.3) | .15 |
| FW, mean (SD) | 22.9 (2.1) | 24.1 (2.5) | 25.3 (2.1) | 25.3 (2.3) | .018* | 22.6 (2.3) | 23.9 (2.7) | 24.8 (2.0) | 25.3 (2.2) | .06 |
| MD^1000, mean (SD) | 7.26 (0.46) | 7.47 (0.43) | 7.83 (0.35) | 7.78 (0.62) | 0.006* | 7.21 (0.52) | 7.41 (0.47) | 7.67 (0.41) | 7.74 (0.53) | 0.044* |
| FA, mean (SD) ^100 | 0.385 (0.028) | 0.367 (0.031) | 0.348 (0.023) | 0.347 (0.037) | 0.003* | 0.386 (0.035) | 0.374 (0.028) | 0.355 (0.030) | 0.353 (0.033) | 0.044* |
| FW-corrected MD ^1000 | 5.58 (0.29) | 5.61 (0.21) | 6.24 (1.00) | 5.87 (0.47) | 0.016* | 5.60 (0.42) | 5.78 (0.89) | 5.91 (0.65) | 5.85 (0.38) | 0.666 |
| FW-corrected FA —^100 | 0.459 (0.030) | 0.441 (0.032) | 0.420 (0.027) | 0.420 (0.041) | 0.004* | 0.458 (0.039) | 0.449 (0.029) | 0.428 (0.033) | 0.426 (0.036) | 0.072* |

WMH ratio: WM hyperintensities/intracranial volume. PVS-BG: periventricular spaces in basal ganglia. PVS-WM: periventricular spaces in WM. SVD: small vessel disease. ALPS: along the perivascular spaces. FW: free water; MD: mean diffusivity. FA: fractional anisotropy. *: P-values <0.05.

**Supplementary table 1**: Sin Mary of the diffusion metric within the normal-appearing WM.

| | MEAN | STD | MIN | MAX | Q25 | Q50 | Q75 |
|---|---|---|---|---|---|---|---|
| **FA** | 0,364611414 | 0,18526427 | 0,015759828 | 0,999094711 | 0,237282745 | 0,358821829 | 0,489986822 |
| **MD** | 0,000755961 | 0,000234254 | 2,17098E-05 | 0,013616231 | 0,000667254 | 0,000713179 | 0,000767823 |
| **Fafw** | 0,438958077 | 0,212632416 | 0,019576292 | 1 | 0,259133 | 0,419512 | 0,593213 |
| **MDFW** | 0,000572352 | 0,000522585 | 1,91878E-06 | 0,086554767 | 0,000507 | 0,000555 | 0,00061 |
| **FW** | 0,253679666 | 0,138165804 | 1,13336E-05 | 0,999965216 | 0,165431 | 0,228865 | 0,29053 |

**Supplementary table 2:** Ordinal regression analyses of each imaging feature using appearance-DMV score and count-DMV score as the dependent variable.

| | Appearance-DMV score | | | Count-DMV score | | |
|---|---|---|---|---|---|---|
| | Unadjusted | Model 1 | Model 2 | Unadjusted | Model 1 | Model 2 |
| | OR (95% CI) | OR (95% CI) | OR (95% CI) | OR (95% CI) | OR (95% CI) | OR (95% CI) |
| **WMH volume (%)** | 1.73* (1.11-2.71) | 1.43 (0.85-2.41) | - | 1.99* (1.21-3.26) | 1.75 (0.98-3.12) | - |
| **PVS-BG volume (%)** | 1.43* (1.01-1.94) | 1.17 (0.81-1.69) | - | 1.22 (0.90-1.65) | 1.19 (0.82-1.75) | - |
| **PVS-WM volume (%)** | 1.29 (0.70-2.41) | 0.95 (0.48-1.87) | - | 1.22 (0.66-2.25) | 1.14 (0.59-2.26) | - |
| **Lacunes, n** | 1.11 (0.88-1.39) | 0.99 (0.77-1.29) | - | 1.26* (1.01-1.58) | 1.16 (0.91-1.48) | - |
| **Microbleeds, n** | 1.09 (0.80-1.51) | 1.09 (0.76-1.55) | - | 1.22 (0.89-1.66) | 1.08 (0.77-1.53) | - |
| **Summary SVD score** | 1.64* (1.06-2.54) | 1.35 (0.81-2.27) | - | 1.65* (1.09-2.48) | 1.31 (0.81-2.12) | - |
| **Brain volume (dL)** | 0.5 (0.31-0.8) | 0.61 (0.32-1.15) | 0.63 (0.33-1.24) | 0.54 (0.35-0.84)* | 0.46 (0.24-0.88)* | 0.48 (0.25-0.94)* |
| **ALPS Index** | 0.83 (0.09-7.65) | 1.18 (0.11-12.18) | 1.28 (0.12-13.39) | 0.39 (0.04-3.75) | 0.47 (0.05-4.66) | 0.51 (0.05-5.15) |
| **FW ^100** | 1.42* (1.12-1.79) | 1.35* (1.06-1.74) | 1.33* (1.03-1.73) | 1.34* (1.07-1.68) | 1.24 (0.98-1.59) | 1.21 (0.94-1.56) |
| **MD ^10000** | 6.90* (2.19-21.79) | 4.90* (1.44-16.67) | 4.56* (1.32-15.81) | 4.84* (1.60-14.58) | 3.78* (1.11-12.91) | 3.45 (0.99-11.94) |
| **FA ^100** | 0.73 (0.6-0.87)* | 0.76 (0.63-0.92)* | 0.77 (0.63-0.93)* | 0.79 (0.67-0.94)* | 0.8 (0.67-0.97)* | 0.82 (0.68-0.99)* |

| | | | | | | | | | | |
|---|---|---|---|---|---|---|---|---|---|---|
| **FW-corrected MD MDfw ^10000** | 2.23 (0.99-5.02) | 2.09 | (0.94-4.64) | 2.39* | (1.06-5.39) | 1.49 (0.64-3.47) | 1.49 | (0.67-3.31) | 1.60 | (0.72-3.56) |
| **FW-corrected FA FAfw ^100** | 0.75 (0.63-0.88)* | 0.78 | (0.65-0.93)* | 0.78 | (0.65-0.94)* | 0.82 (0.7-0.95)* | 0.88 | (0.69-0.98)* | 0.83 | (0.7-0.99)* |

Model 1 includes age, sex, and cigarettes/day. Model 2 includes Model 1 plus summary SVD score. WMH ratio: WM hyperintensities/intracranial volume. PVS-BG: periventricular spaces in basal ganglia. PVS-WM: periventricular spaces in WM. SVD: small vessel disease. ALPS: along the perivascular spaces. FW: free water. MD: mean diffusivity. FA: fractional anisotropyOR: Odds ratio. *P value <.05

**Supplementary table 3:** STROBE Statement—checklist of items that should be included in reports of observational studies.

| | Item No. | Recommendation | Page No. | Relevant text from manuscript |
|---|---|---|---|---|
| **Title and abstract** | 1 | (*a*) Indicate the study's design with a commonly used term in the title or the abstract | 1 | "After categorizing the cohort…" |
| | | (*b*) Provide in the abstract an informative and balanced summary of what was done and what was found | 1 | "In univariate analysis…" |
| **Introduction** | | | | |
| **Background/rationale** | 2 | Explain the scientific background and rationale for the investigation being reported | 2 | "Cerebral small vessel disease (SVD) primarily affects small penetrating arteries, capillaries, and veins.." |
| **Objectives** | 3 | State specific objectives, including any prespecified hypotheses | 2 | "We hypothesize that DMV alterations assessed by their appearance and count on SWI …" |
| **Methods** | | | | |
| **Study design** | 4 | Present key elements of study design early in the paper | 2 | "This is a post-hoc cross-sectional analysis of, a prospective cohort study focused on …" |
| **Setting** | 5 | Describe the setting, locations, and relevant dates, including periods of recruitment, exposure, follow-up, and data collection | 2 | "Fifty patients with a recent small subcortical infarct were admitted between June 2022 and March 2023 and…" |
| **Participants** | 6 | (*a*) *Cohort study*—Give the eligibility criteria, and the sources and methods of selection of participants. Describe methods of follow-up<br>*Case-control study*—Give the eligibility criteria, and the sources and methods of case ascertainment and control selection. Give the rationale for the choice of cases and controls<br>*Cross-sectional study*—Give the eligibility criteria, and the sources and methods of selection of participants<br>(*b*) *Cohort study*—For matched studies, give matching criteria and number of exposed and unexposed<br>*Case-control study*—For matched studies, give matching criteria and the number of controls per case | 2 | "The presence of a recent small subcortical infarct confirmed on DWI sequences according to the STandards for ReportIng Vascular changes on nEuroimaging (STRIVE) criteria…" |
| **Variables** | 7 | Clearly define all outcomes, exposures, predictors, potential confounders, and effect modifiers. Give diagnostic criteria, if applicable | 2 | "The collected variables included age, sex, number of cigarettes per day, history of hypertension, |

| | | | | |
|---|---|---|---|---|
| | | | | diabetes and hyperlipidemia…" |
| **Data sources/ measurement** | 8* | For each variable of interest, give sources of data and details of methods of assessment (measurement). Describe comparability of assessment methods if there is more than one group | 2,3 | "Visual assessment of DMV on MRI…" "SVD assessment on MRI…" "Brain diffusivity analysis…" |
| **Bias** | 9 | Describe any efforts to address potential sources of bias | 2,3 | "All MRI studies were acquired …" "After training…" |
| Study size | 10 | Explain how the study size was arrived at | 2 | "This is a post-hoc cross-sectional analysis of, a prospective cohort study.." |
| Quantitative variables | 11 | Explain how quantitative variables were handled in the analyses. If applicable, describe which groupings were chosen and why | 3 | "Given the skewed distribution of DMV scores, we stratified the cohort into DMV scores quartiles…" |
| Statistical methods | 12 | (*a*) Describe all statistical methods, including those used to control for confounding | 3 | "To assess inter-rater reliability…" "For the cohort description…" |
| | | (*b*) Describe any methods used to examine subgroups and interactions | 3 | "Given the skewed distribution of DMV scores, we stratified the cohort into DMV scores quartiles…" |
| | | (*c*) Explain how missing data were addressed | 5 | "All fifty patients had complete data, including suitable SWI sequences" |
| | | (*d*) *Cohort study*—If applicable, explain how loss to follow-up was addressed<br>*Case-control study*—If applicable, explain how matching of cases and controls was addressed<br>*Cross-sectional study*—If applicable, describe analytical methods taking account of sampling strategy | | NA |
| | | (*e*) Describe any sensitivity analyses | 3 | "Model 1 included age, sex, and cigarette number; Model 2 added summary-SVD score to Model 1" |
| Results | | | | |
| Participants | 13* | (a) Report numbers of individuals at each stage of study—eg numbers potentially eligible, examined for eligibility, confirmed eligible, included in the study, completing follow-up, and analysed | | |
| | | (b) Give reasons for non-participation at each stage | 2 | "This is a post-hoc cross-sectional analysis of, a prospective cohort study.." |
| | | (c) Consider use of a flow diagram | | NA |
| Descriptive data | 14* | (a) Give characteristics of study participants (eg demographic, clinical, social) and information on exposures and potential confounders | 5 | "Most of the participants had history of hypertension (62%) and hyperlipidemia (58%), and seventeen (34%) had diabetes mellitus…" |
| | | (b) Indicate number of participants with missing data for each variable of interest | | |
| | | (c) *Cohort study*—Summarise follow-up time (eg, average and total amount) | | |
| Outcome data | 15* | *Cohort study*—Report numbers of outcome events or summary measures over time<br>*Case-control study*—Report numbers in each exposure category, or summary measures of exposure | | |
| | | *Cross-sectional study*—Report numbers of outcome events or summary measures | 5 | "The intraclass correlation coefficient for the appearance-DMV score…" |
| Main results | 16 | (*a*) Give unadjusted estimates and, if applicable, confounder-adjusted estimates and their precision (eg, 95% confidence interval). Make clear which confounders were adjusted for and why they were included | | |
| | | (*b*) Report category boundaries when continuous variables were categorized | | Appereance-DMV 3-18<br>Count-DMV 1-18 |
| | | (*c*) If relevant, consider translating estimates of relative risk into absolute risk for a meaningful time period | | NA |
| Other analyses | 17 | Report other analyses done—eg analyses of subgroups and interactions, and sensitivity analyses | | NA |

| | | | | |
|---|---|---|---|---|
| Discussion | | | | |
| Key results | 18 | Summarise key results with reference to study objectives | 6 | "…align with previous evidence that DMV integrity may be linked to other SVD features(8-15)…" |
| Limitations | 19 | Discuss limitations of the study, taking into account sources of potential bias or imprecision. Discuss both direction and magnitude of any potential bias | 7 | "Firstly, the small sample size might…" |
| Interpretation | 20 | Give a cautious overall interpretation of results considering objectives, limitations, multiplicity of analyses, results from similar studies, and other relevant evidence | 7 | "Further research is needed…" |
| Generalisability | 21 | Discuss the generalisability (external validity) of the study results | 3,7 | "…according to STRIVE criteria."<br>"…protocols were set up according to HARNESS…" |
| Other information | | | | |
| Funding | 22 | Give the source of funding and the role of the funders for the present study and, if applicable, for the original study on which the present article is based | 9 | "Project funded by the Catalan Society of Neurology…" |

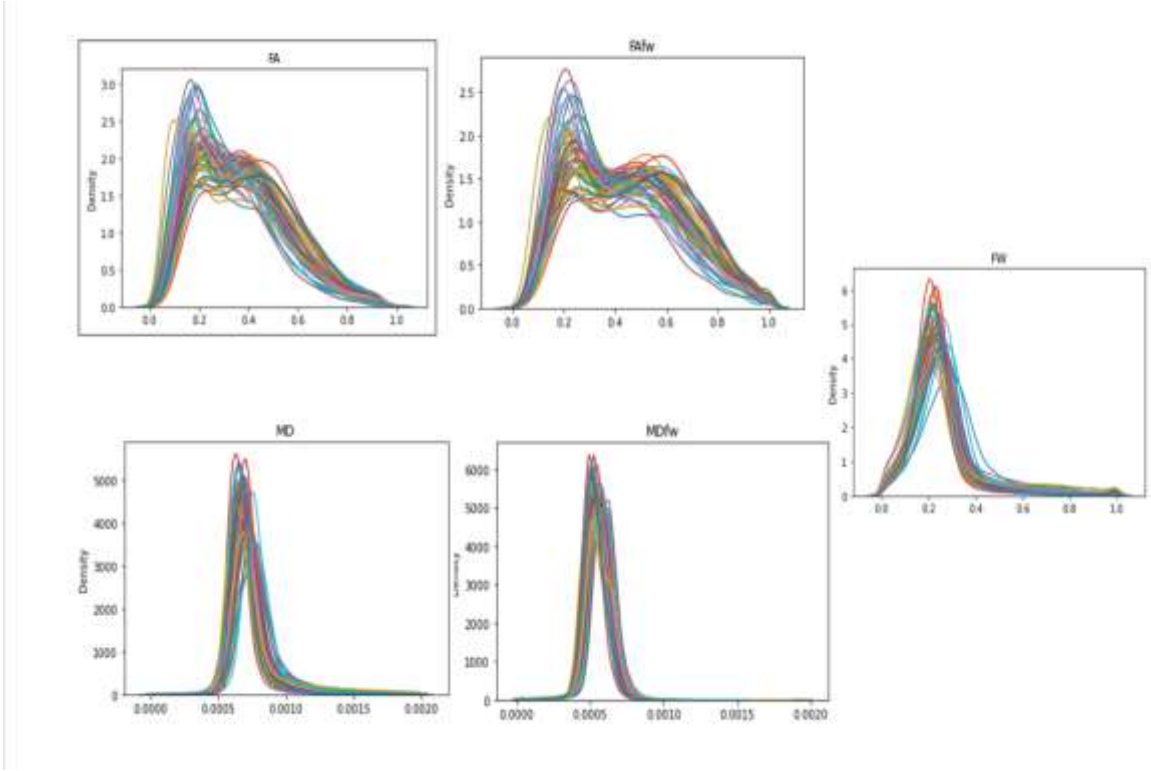


**SUPPLEMENTARY FIG 1.** The distribution of diffusion parameters in normal-appearing WM follows a consistent pattern across all subjects. For mean diffusivity (MD), free-water corrected mean diffusivity (MDfw), and free-water (FW), the values within the NAWM fall within a narrow range. In contrast, while the fractional anisotropy (FA) values show a broader range of variation within normal-appearing WM regions, the overall distribution of these values remains consistent across all subjects in the dataset.

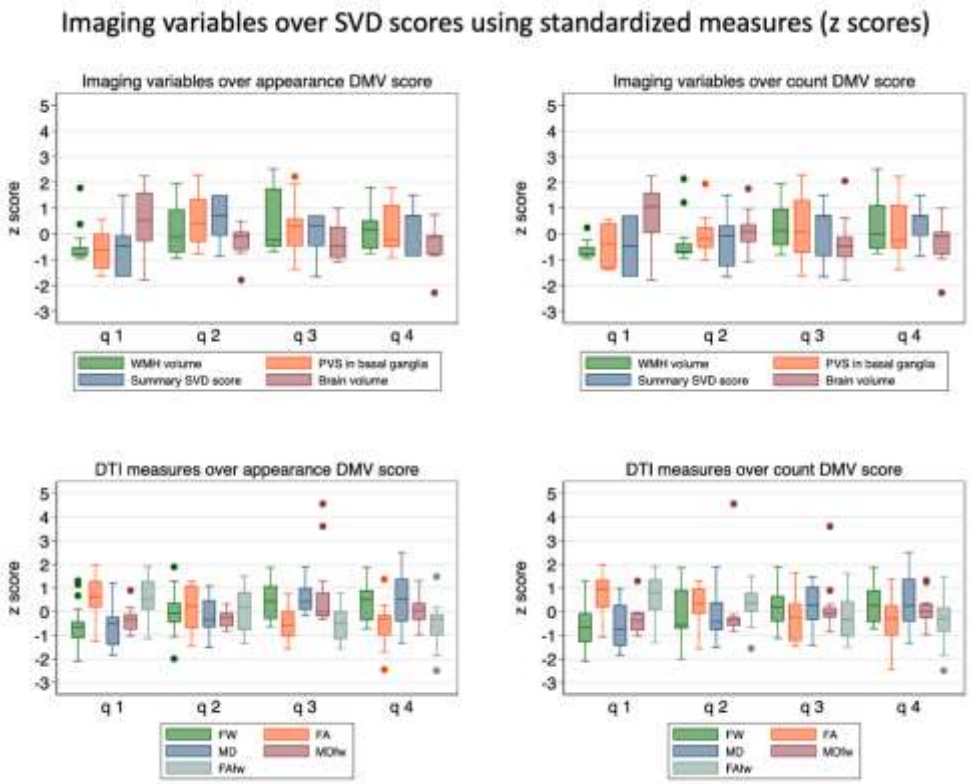


**SUPPLEMENTARY FIG 2.** Box plots of the most relevant distributions in the descriptive analysis of radiological variables according to the appearance-DMV score quartiles and count-DMV.